maximum uncertainty (Fig. 1 and fig. S1). For example, increased breakdown rates in slightly enriched streams would indicate altered ecosystem functioning, although most managers would consider such streams ecologically intact on the basis of traditional assessment criteria. Conversely, low breakdown rates at moderately enriched sites are no guarantee that streams are unaffected, requiring comprehensive assessments based on a range of indicators in order to draw conclusions about ecosystem impairment.

Our results raise fundamental questions about how to determine ecosystem health. First, naturally low-nutrient conditions are the desired state that water resource managers aspire to, and yet breakdown rates in such systems were indistinguishable from those in heavily polluted streams. This suggests that ensuring both low-nutrient water and effective resource use in stream food webs (from leaf litter to detritivores to fish) coupled with high process rates might be irreconcilable goals in stream management. Second, stream managers currently rely primarily on structural measures to assess stream ecosystem health. In particular, changes in biological community structure (invertebrates, fish, and algae) have long underpinned stream bioassessment schemes because they provide a reliable time-integrated response to stressors such as organic pollution or acidification (*5*), but biogeographical constraints make this approach difficult to standardize at large scales (*10*). Litter breakdown can help here because biogeography is a minor issue (for example, black alder or similar species of the genus are common throughout most of Europe and the Holarctic), and marked changes in breakdown rate occurred in the rising portion of the pollution gradient, in which established structural measures (such as water chemistry, hydromorphology, and metrics based on fish, invertebrate, or algal communities) are typically least sensitive. Consequently, litter breakdown—and potentially other functional measures such as whole-ecosystem metabolism, nutrient spiraling, or primary production (*26*–*28*)—can be used to complement, not replace, established procedures to assess stream ecosystem health. This highlights the need for differential diagnoses in environmental assessment, as is standard practice in medicine. Importantly, litter breakdown and some other functionally based methods can be implemented at relatively little cost or resource input (*29*) in order to assess effects of pollution and other ecosystem impacts that are of concern to environmental managers and stakeholders.

Increasing human pressure is accelerating environmental change throughout the world, threatening water security for humans and aquatic biodiversity (*2*). Large stretches of the landscape in Europe and other parts of the world are characterized today by highly industrialized, intensively managed agriculture and the large-scale application of fertilizers. This, in combination with other nutrient sources such as atmospheric deposition, has resulted in widespread nutrient pollution of aquatic ecosystems (*2*, *5*, *8*). Our study reveals that along with biodiversity losses, as fresh waters drift away from their natural conditions, ecosystem processes are profoundly changed, too. Impacts on stream functioning may go beyond the effects on litter breakdown because changing litter dynamics can have strong effects on nutrient retention and transformations (*27*), invertebrate productivity (*12*, *30*), and other functional ecosystem attributes. Given these complexities and large uncertainties surrounding human environmental impacts (*5*, *24*), a critical objective for the future will be to improve concepts and implementation tools to simultaneously manage surface waters sustainably and meet the demands of biodiversity conservation and environmental legislation.

References and Notes

1. A. M. Helton *et al.*, *Front. Ecol. Environ* **9**, 229 (2011).
2. C. J. Vörösmarty *et al.*, *Nature* **467**, 555 (2010).
3. E. S. Bernhardt *et al.*, *Science* **308**, 636 (2005).
4. P. H. Gleick, *Science* **302**, 1524 (2003).
5. N. Friberg *et al.*, *Adv. Ecol. Res* **44**, 2 (2011).
6. D. Hering *et al.*, *Sci. Total Environ.* **408**, 4007 (2010).
7. M. O. Gessner, E. Chauvet, *Ecol. Appl.* **12**, 498 (2002).
8. J. Hilton, M. O'Hare, M. J. Bowes, J. I. Jones, *Sci. Total Environ.* **365**, 66 (2006).
9. C. Perrings *et al.*, *Science* **330**, 323 (2010).
10. M. O. Gessner *et al.*, *Trends Ecol. Evol.* **25**, 372 (2010).
11. J. C. Moore *et al.*, *Ecol. Lett.* **7**, 584 (2004).
12. J. B. Wallace, S. L. Eggert, J. L. Meyer, J. R. Webster, *Science* **277**, 102 (1997).
13. J. L. Tank, E. J. Rosi-Marshall, N. A. Griffiths, S. A. Entrekin, M. L. Stephen, *J. N. Am. Benthol. Soc.* **29**, 118 (2010).
14. J. R. Webster, E. F. Benfield, *Annu. Rev. Ecol. Syst.* **17**, 567 (1986).
15. V. Gulis, K. Suberkropp, *Freshw. Biol.* **48**, 123 (2003).
16. A. D. Rosemond, C. M. Pringle, A. Ramírez, M. J. Paul, J. L. Meyer, *Limnol. Oceanogr.* **47**, 278 (2002).
17. C. F. Mason, *Biology of Freshwater Pollution* (Prentice-Hall, Upper Saddle River, NJ, ed. 4, 2002), p. 391.
18. M. Bundschuh, T. Hahn, M. O. Gessner, R. Schulz, *Environ. Toxicol. Chem.* **28**, 197 (2009).
19. M. Hieber, M. O. Gessner, *Ecology* **83**, 1026 (2002).
20. C. Pascoal, M. Pinho, F. Cassio, P. Gomes, *Freshw. Biol.* **48**, 2033 (2003).
21. Materials and methods are available as supplementary materials on *Science* Online.
22. C. J. F. ter Braak, P. Smilauer, *CANOCO Reference Manual and User's Guide to CANOCO for Windows: Software for Canonical Community Ordination* (Microcomputer Power, Ithaca, NY, 1998).
23. A. Lecerf *et al.*, *Arch. Hydrobiol.* **165**, 105 (2006).
24. L. Boyero *et al.*, *Ecol. Lett.* **14**, 289 (2011).
25. S. Hladyz *et al.*, *Adv. Ecol. Res* **44**, 211 (2011).
26. R. G. Young, K. J. Collier, *Freshw. Biol.* **54**, 2155 (2009).
27. P. J. Mulholland, J. R. Webster, *J. N. Am. Benthol. Soc.* **29**, 100 (2010).
28. P. J. Mulholland *et al.*, *Nature* **452**, 202 (2008).
29. M. J. Feio, T. Alves, M. Boavida, A. Medeiros, M. A. S. Graça, *Freshw. Biol.* **55**, 1050 (2010).
30. W. F. Cross, J. B. Wallace, A. D. Rosemond, S. L. Eggert, *Ecology* **87**, 1556 (2006).

Acknowledgments: We thank the European Commission and the Swiss State Secretariat for Research and Education for funding the RivFunction research project (European Union contract EVK1-CT-2001-00088), which was supported under the Fifth Framework Programme. The constructive comments by three anonymous reviewers, which substantially improved the paper, are greatly appreciated. All basic data are available in the supplementary materials. This paper is dedicated to the memory of our colleague Björn Malmqvist, who sadly passed away in 2010.

Supplementary Materials

www.sciencemag.org/cgi/content/full/336/6087/1438/DC1
Materials and Methods
Figs. S1 to S6
Table S1
Reference (*31*)
Databases S1 and S2

23 January 2012; accepted 26 April 2012
10.1126/science.1219534

p53 Dynamics Control Cell Fate

Jeremy E. Purvis, Kyle W. Karhohs, Caroline Mock, Eric Batchelor,* Alexander Loewer,† Galit Lahav‡

Cells transmit information through molecular signals that often show complex dynamical patterns. The dynamic behavior of the tumor suppressor p53 varies depending on the stimulus; in response to double-strand DNA breaks, it shows a series of repeated pulses. Using a computational model, we identified a sequence of precisely timed drug additions that alter p53 pulses to instead produce a sustained p53 response. This leads to the expression of a different set of downstream genes and also alters cell fate: Cells that experience p53 pulses recover from DNA damage, whereas cells exposed to sustained p53 signaling frequently undergo senescence. Our results show that protein dynamics can be an important part of a signal, directly influencing cellular fate decisions.

Cells use molecular signaling networks to sense, interpret, and respond to stimuli. Recent advances in time-lapse microscopy have revealed that many signaling molecules show complex dynamical behaviors (*1*–*13*). In some instances, dynamical properties such as oscillation frequency or signal duration, have been shown to alter gene expression (*1*, *3*, *6*, *8*, *11*, *13*–*16*) or to control cellular differentiation (*7*, *12*, *17*). These examples point to a rich mode of regula-

tion that is largely unexplored for most biological pathways. We developed a mathematically designed perturbation of p53 dynamics in response to DNA damage and have shown experimentally that p53 dynamics determine cellular responses.

p53 is a tumor suppressor activated in response to cellular stress (*18*, *19*). Induction of p53 triggers multiple cellular programs ranging from transient responses, such as DNA repair and cell cycle arrest, to terminal fates such as cell death (apoptosis) and permanent cell cycle arrest (senescence) (Fig. 1A). Recently, it was shown that different stresses evoke different dynamic patterns of p53 protein levels (Fig. 1B) (*20*). In response to DNA breaks caused by γ-irradiation, the levels of p53 exhibit a series of pulses with fixed amplitude and frequency (*4*, *21*). Higher radiation doses increase the number of pulses without affecting their amplitude or duration. These p53 pulses were observed in a live mouse model (*22*) and in various transformed and non-transformed human cell lines (*23*–*25*). In contrast, ultraviolet (UV) radiation triggers a single p53 pulse with a dose-dependent amplitude and duration (*20*). Although much insight has been gained into the molecular mechanisms that control these differential p53 dynamics in response to γ and UV radiation (*20*, *25*, *26*), the effect of p53 dynamics on downstream responses remains unknown. UV and γ radiation activate distinct targets of p53 (*27*) and lead to different cellular outcomes (Fig. 1B), suggesting that downstream elements in the p53 network may respond to the dynamic profiles of p53. However, γ and UV radiation also lead to many p53-independent events in cells, which could contribute to the differential outcomes. A definitive conclusion about the role of p53 dynamics on cellular outcomes may come from experimentally perturbing p53 dynamics in response to the same stress and observing the effect on downstream responses.

We developed a method for altering p53 dynamics after γ-irradiation. Our goal was to switch p53 natural pulses into a sustained p53 signal held at the peak pulse amplitude (Fig. 1C). We used the small molecule Nutlin-3, which binds to the p53 inhibitor Mdm2, inhibiting degradation of the p53 protein (*28*). Nutlin-3 is selective for p53 because $p53^{-/-}$ cells show no change in genome-wide expression profiling upon Nutlin-3 treatment (*29*). Achieving a sustained signaling response with a single Nutlin-3 treatment proved to be difficult: *MDM2* is activated by p53, and therefore, addition of Nutlin-3 not only stabilizes p53 but also causes an increase in Mdm2 levels that eventually overcomes Nutlin-3 inhibition, resulting in down-regulation of p53 (fig. S1). Treatment with a higher dose of Nutlin-3 led to prolonged induction of p53 but also to an overshoot in p53 levels (fig. S1). To overcome this obstacle, we trained our model of p53 dynamics (*26*) to predict the optimal sequence of Nutlin-3 additions necessary to sustain p53 at a constant level (Fig. 1D, fig. S2, and tables S1 and S2). The model predicted that three sequential treatments of Nutlin-3 at 2.5 hours (0.75 μM), 3.5 hours (2.25 μM), and 5.5 hours (4 μM) after γ-irradiation would produce a sustained p53 response with an amplitude equal to p53 natural pulses. This prediction was validated experimentally in both cell populations and single cells (Fig. 1E and fig. S3). These two dynamical "inputs"—naturally pulsed and pharmacologically sustained p53 signaling (hereafter, "pulsed" and "sustained")—were then used to study the downstream effects of p53 dynamics on target gene expression and cellular outcome.

Department of Systems Biology, Harvard Medical School, Boston, MA 02115, USA.

*Present address: Laboratory of Pathology, National Cancer Institute, National Institutes of Health, Bethesda, MD 20892, USA.

†Present address: Berlin Institute for Medical Systems Biology, Max Delbrueck Center for Molecular Medicine, Berlin-Buch 13125, Germany.

‡To whom correspondence should be addressed. E-mail: galit@hms.harvard.edu

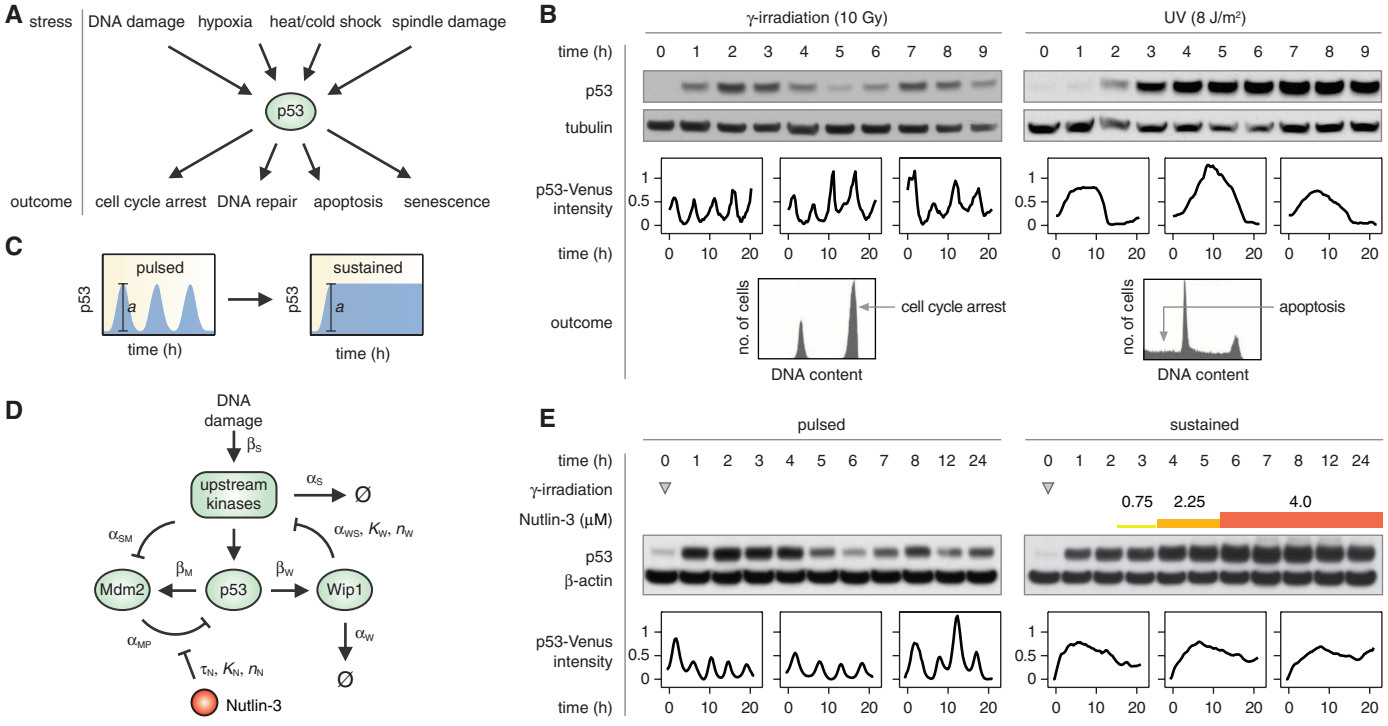

Fig. 1. Perturbation of p53 dynamics. (**A**) p53 mediates the response to multiple cellular stresses and evokes diverse cellular outcomes. (**B**) γ-irradiation leads to p53 pulses and cell cycle arrest; UV radiation induces a single prolonged pulse and leads to apoptosis. (**C**) p53's natural pulses were perturbed to produce a sustained response with equal amplitude, *a*. (**D**) A diagram capturing the main species and parameters in the mathematical model of p53 dynamics after DNA damage (*26*). This model was used to predict the optimal sequence of Nutlin-3 additions needed to generate a sustained p53 response after γ-irradiation (supplementary materials). (**E**) p53 dynamics under (left) naturally pulsed or (right) pharmacologically sustained conditions. The sequence of Nutlin-3 treatments is denoted by differently colored bars. Pulses in immunoblots appear as damped oscillations because of the asynchronous responses of single cells. Representative single-cell traces show average nuclear p53-Venus intensities that were normalized to the median value and zeroed to the minimum value. Sequential Nutlin-3 treatment did not alter the amplitude of p53 (fig. S3).

To understand how p53 dynamics control gene expression, we selected a panel of well-studied p53 target genes representing different functional pathways and cellular outcomes (*30*). A subset of genes showed a clear oscillatory response that mirrored p53 protein dynamics (Fig. 2, A and B, and table S3). This group included genes involved in cell cycle arrest and DNA repair (*CDKN1A*, *GADD45A*, and *XPC*), as well as genes known to regulate p53 levels (*MDM2* and *PPM1D*). In contrast, transcripts encoding apoptotic proteins (*APAF1*, *BAX*, and *TP53AIP*) or involved in p53-dependent senescence (*PML* and *YPEL3*) (*31*, *32*) were not induced by p53 pulses (Fig. 2, C and D).

We next measured expression of these transcripts using our dynamic drug treatment (Fig. 1E) to sustain p53 signaling. Oscillating genes (such as *MDM2* and *CDKN1A*) showed sustained increases in expression. Genes involved in apoptosis or senescence—which were not induced by p53 pulses—showed either no induction (*APAF1* and *TP53AIP1*) or a delayed increase in expression (*BAX*, *PML*, and *YPEL3*) under sustained p53 signaling. These trends were p53-dependent (fig. S4). Taken together, these results indicate that p53 pulses selectively activate genes involved in transient responses to DNA damage, whereas sustained p53 signaling allows induction of genes associated with terminal fates.

We next asked whether changes in p53 dynamics lead to different cell fates—specifically, whether sustained p53 will trigger irreversible fates such as apoptosis or senescence, whereas pulsed p53 will allow recovery and growth. DNA content analysis by means of flow cytometry revealed only a small amount of cell death under both pulsed and sustained p53 conditions (fig. S5). We therefore pursued the alternate possibility that sustained p53 signaling promotes cellular senescence, a state of permanent cell cycle arrest (*33*, *34*). Cells were subjected to pulsed or sustained p53 signaling at several γ-irradiation doses and then assayed for senescence-associated β-galactosidase (β-gal) activity and their ability to proliferate in fresh growth media (fig. S6). At lower doses of γ-irradiation [2.5 and 5 grays (Gy)], sustained p53 signaling led to large increases in β-gal–positive cells (Fig. 3, A and B). At these levels of DNA damage, the majority of cells exposed to pulsed p53 were able to undergo multiple rounds of growth and division after recovery (Fig. 3, C to E, and fig. S7), whereas sustained p53 signaling reduced this fraction substantially, leading to a characteristically flattened morphology and an apparent inability to divide (Fig. 3C). These differences were most pronounced after 5 Gy of γ-irradiation—a dose at which nearly all cells showed a permanent arrest after sustained p53 signaling (Fig. 3, D and E). Sustained p53 signaling at 2.5 Gy led to a greater fraction of senescent cells than did pulsed p53 at 5 Gy (Fig. 3, B and E), suggesting that it is not the extent of DNA damage that induces senescence, but rather the dynamics of p53 signaling.

We did not observe a large difference in β-gal activity or in proliferative ability at the highest dose of γ-irradiation (10 Gy). This suggested that prolonged p53 pulsing (*4*, *21*, *25*) caused by extensive DNA damage might eventually lead to expression of senescence genes. Indeed, we found that after 3 days under pulsed conditions, the p53-dependent senescence genes were induced to similar levels reached under sustained conditions after 1 day (Fig. 3F). *CDKN1A*, which is involved in both cell cycle arrest and p53-dependent senescence (*33*, *34*), showed the most dramatic increase in expression (>100-fold) under sustained p53 signaling.

Thus, sustained p53 signaling appears to accelerate the expression of senescence genes, whereas pulsed p53 delays gene expression and so protects cells from prematurely committing to an irreversible fate. However, by the time a cell commits to senescence the total amount of p53 accumulated over time ("cumulative p53") is

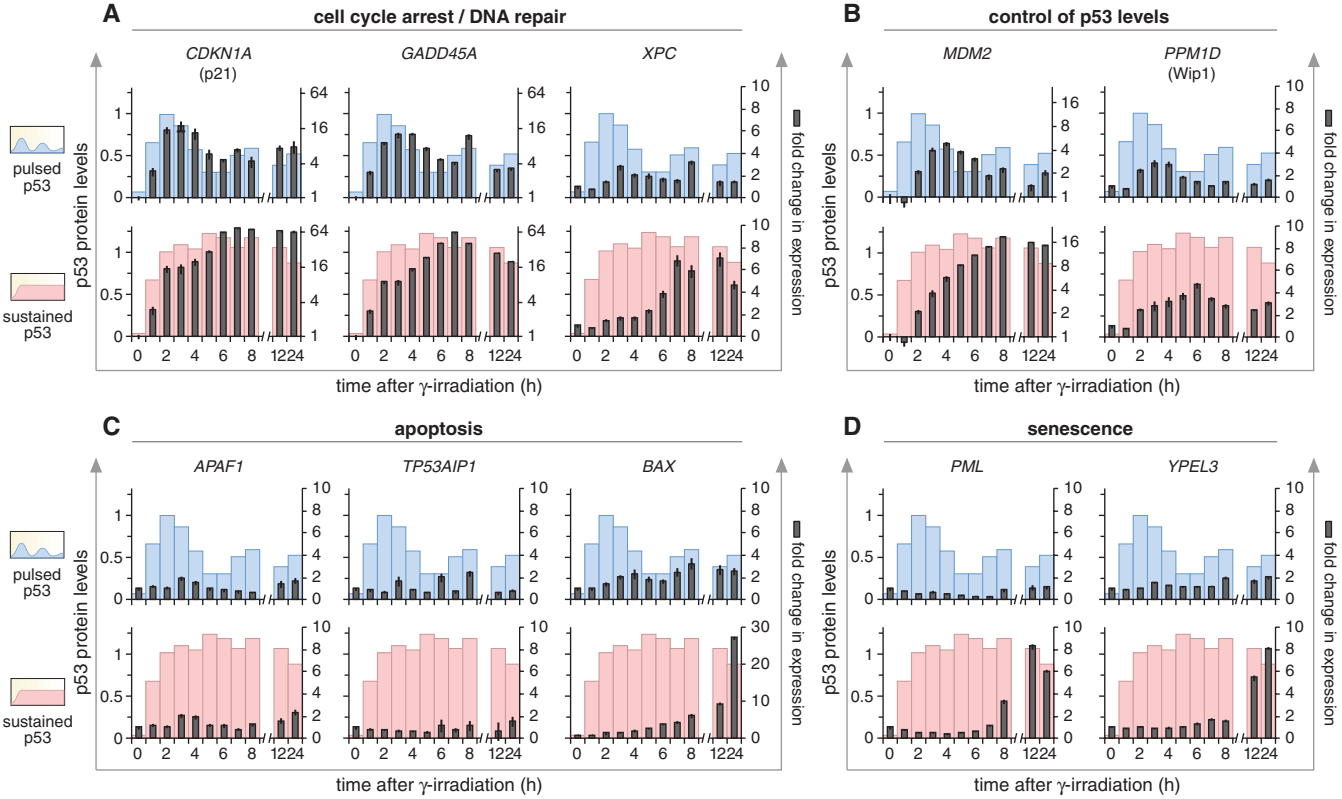

Fig. 2. Pulsed and sustained p53 signaling activate different sets of target genes. Expression of p53 target genes was measured under pulsed or sustained conditions after γ-irradiation. Genes are grouped according to function: (**A**) cell cycle arrest and DNA repair, (**B**) control of p53 levels, (**C**) apoptosis, and (**D**) senescence. For reference, p53 protein levels are shown in the background as light blue (pulsed) or red (sustained) bars. p53 levels are normalized to the peak (t = 2 hours) p53 concentration. A base-2 logarithmic scale is used for *CDKN1A*, *GADD45A*, and *MDM2*. Data are mean ± SD. Significance of correlation between target genes and p53 protein levels under pulsed conditions is reported in table S3.

much higher under sustained conditions than in pulsing cells. To determine whether this change in cell fate is due to p53 dynamics or merely to an increase in cumulative p53, we compared expression of senescence genes between pulsed and sustained p53 at equivalent levels of cumulative p53 (Fig. 4A). We found that even for similar cumulative p53, sustained p53 signaling led to higher expression of its target genes than pulsed p53, suggesting that it is the dynamics of p53 rather than its accumulated levels that control gene expression.

We further tested this in single cells. We first showed that individual senescent cells have significantly higher levels of *CDKN1A* and *PML* transcripts than those of proliferating cells (fig. S8), confirming that these transcripts are reliable markers for the induction of senescence. We then quantified p53 dynamics under pulsed and sustained conditions and used fluorescence in situ hybridization (FISH) to compare the level of *CDKN1A* and *PML* (Fig. 4, B and C). To achieve comparable cumulative p53 levels between pulsed and sustained p53, we terminated pulsed p53 21 hours after irradiation (t_1) and sustained p53 12 hours after irradiation (t_2) (Fig. 4D). We found that expression of both *CDKN1A* and *PML* was significantly higher under sustained p53 than under pulsed p53 even at similar cumulative p53 levels (Fig. 4, E and F). These results suggest that the decision of whether and when to enter senescence is communicated to cells through the temporal pattern of p53 (Fig. 4G).

It is well established that different posttranslational modifications of p53 or different cofactors that bind p53 affect the choice of downstream gene programs (*35*). Here, we have shown another mechanism for specificity in this network: the dynamics of p53. Our work suggests that p53 dynamics are important but do not act alone: p53 signaling produced by γ-irradiation and Nutlin-3 leads to senescence, whereas a comparable dynamical profile in response to UV radiation leads to apoptosis (Fig. 1B). Future studies are required to explore the combined effect of p53 dynamics and modifications on cellular outcomes.

What molecular mechanism may decode p53 dynamics to determine cell fate? One hypothesis is that p53 pulses periodically exceed a threshold concentration for transcriptional activation of senescence genes. In this scenario, sustained p53 or a greater number of p53 pulses increases the probability that p53 will activate downstream targets that are involved in the induction of senescence. A similar mechanism was previously reported (*14*), in which the frequency of calcium oscillations controls specificity for activation of proinflammatory transcription factors. Another plausible mechanism involves a feed-forward loop motif that discriminates transient and persistent p53 signaling. This type of mechanism was identified in the extracellular signal-related kinase (ERK) signaling pathway, in which the early gene product c-Fos functions as a sensor for sustained ERK levels (*17*). By analogy, an early gene induced by p53 and essential for activating senescence with p53 may decay with a time scale close to the time scale of p53 pulses and therefore accumulates slowly during p53 pulses, but more rapidly during a sustained p53 response. It is also possible that expression of senescence genes is initially repressed, for example, by epigenetic silencing or antisense RNA, and that these factors are deactivated by persistent p53 signaling.

Other signaling pathways have been shown to encode information through the dynamics of their signaling molecules (*1*–*3*, *5*–*13*), suggesting that varying protein dynamics may offer a functional advantage in certain contexts. For example, information encoded in the dynamics, rather than the absolute concentration of a signaling molecule, may be less sensitive to spontaneous fluctuations in the cellular environment. In addition, certain dynamical patterns may allow neighboring cells to synchronize their responses to produce emergent multicellular behaviors. A better understanding of how signaling dynamics are regulated and how they affect cellular responses will provide new insights for manipulating them in a controlled way. In addition, targeted perturbation of protein dynamics, such as the one illustrated in this study, may enable new pharmacological strategies for altering cell fate in a range of diseases.

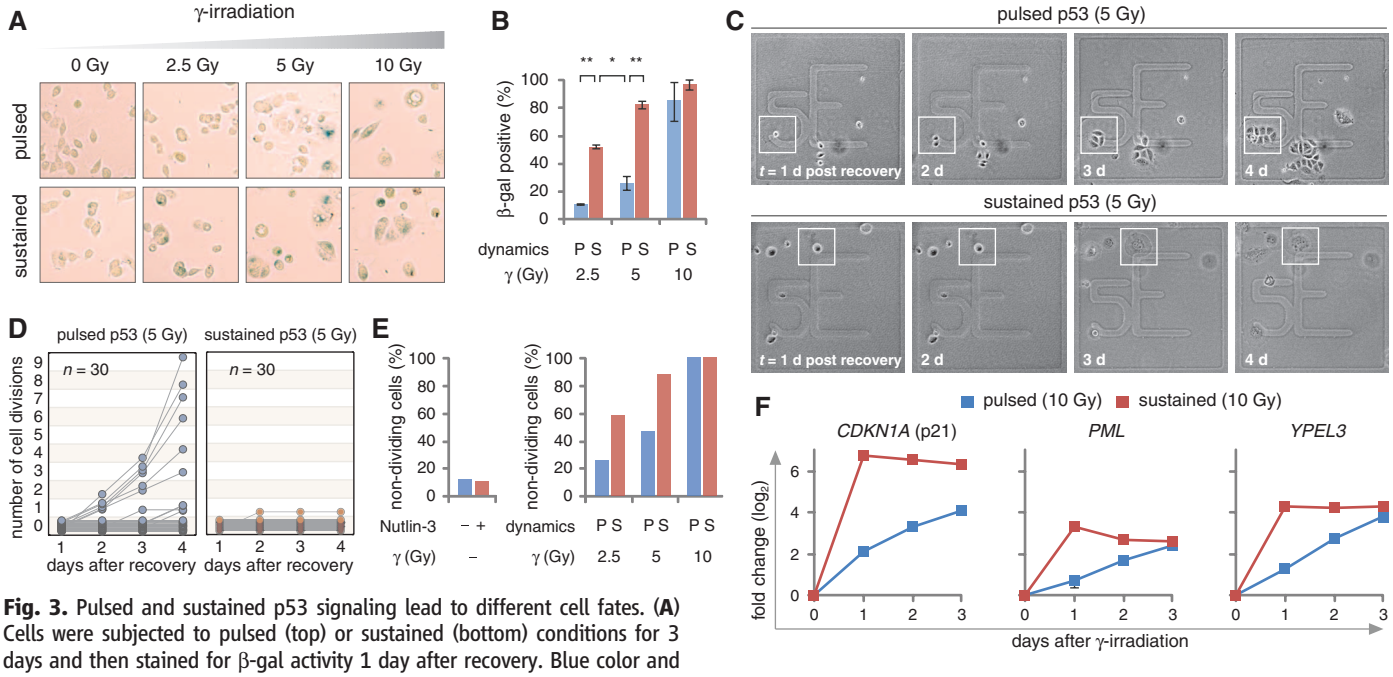

Fig. 3. Pulsed and sustained p53 signaling lead to different cell fates. (**A**) Cells were subjected to pulsed (top) or sustained (bottom) conditions for 3 days and then stained for β-gal activity 1 day after recovery. Blue color and flattened morphology are indicative of senescence. (**B**) Percentage of β-gal-positive cells under pulsed (P) or sustained (S) p53 signaling at various γ-irradiation doses. $n \geq 100$ cells per condition per experiment. *$P < 0.05$, **$P < 0.01$. (**C**) Typical images of single cells that were recovered after 3 days of pulsed (top) or sustained (bottom) p53 signaling at 5 Gy γ-irradiation. White boxes are drawn to show the fate of an individual cell. (**D**) Number of cell divisions for single cells after recovery from pulsed or sustained p53 signaling at 5 Gy. (**E**) (Left) Percentage of cells that did not divide under resting conditions or sequential Nutlin-3 treatment alone (no γ-irradiation). (Right) Percentage of nondividing cells under pulsed (P) or sustained (S) p53 signaling. (**F**) Fold change in expression of *CDKN1A*, *PML*, and *YPEL3* after 24, 48, and 72 hours under pulsed (blue) or sustained (red) p53 signaling (10 Gy γ-irradiation). Expression levels were normalized to *ACTB*. Data are mean ± SD.

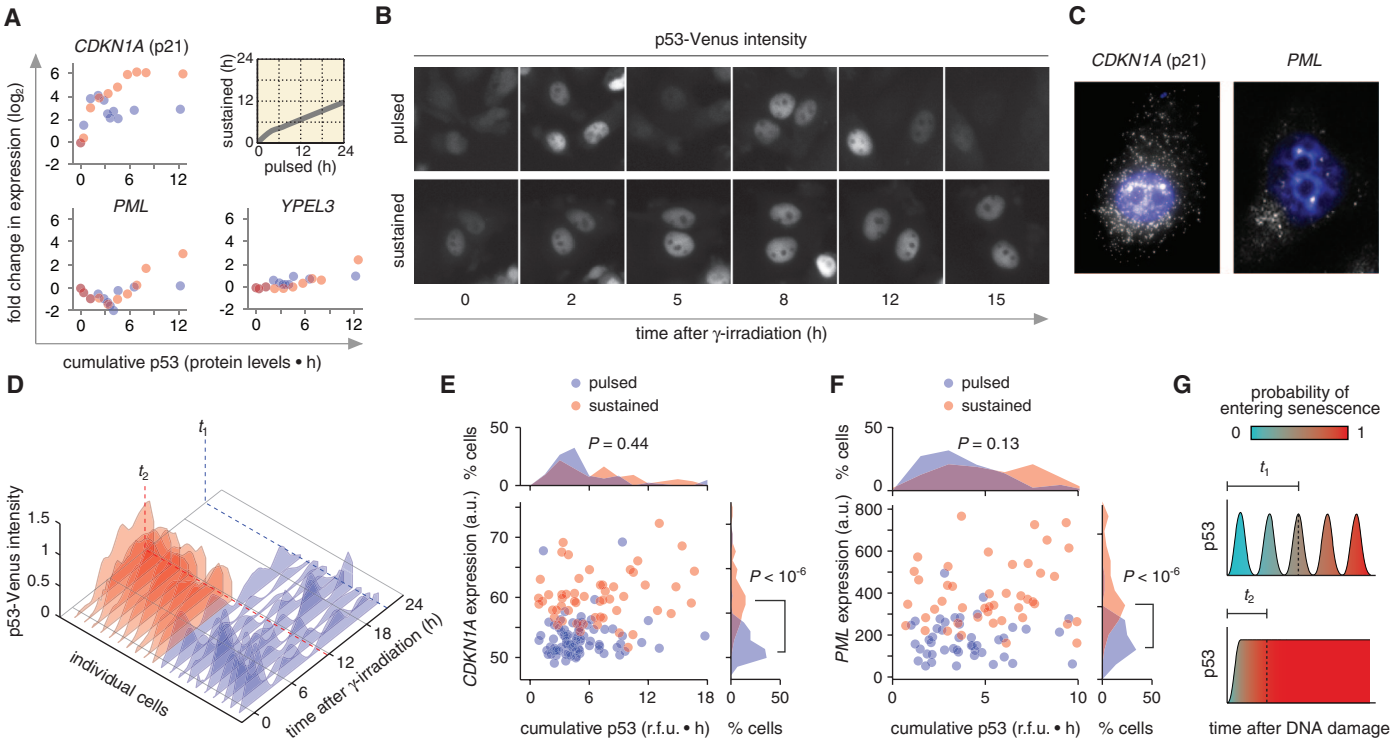

Fig. 4. p53 dynamics, and not its cumulative level, control cell fate. (**A**) (Inset) Time points for which pulsed and sustained p53 signaling show equivalent cumulative p53 levels [$\int p53(t)dt$] lie along the gray line. Gene expression under pulsed (blue dots) or sustained (red dots) p53 signaling are plotted as a function of cumulative p53 by using the data presented in Fig. 1E. The time integral of p53 protein levels was computed by using trapezoidal integration of p53 levels over time. Gene expression was normalized to *ACTB*. The last time point in sustained conditions (24 hours) was omitted because there is no comparable data point under pulsed conditions. (**B**) p53 dynamics were recorded by means of live-cell microscopy under pulsed and sustained conditions. (**C** and **D**) Representative single-cell traces of p53 levels under (blue) pulsed or (red) sustained conditions. Time-lapse imaging was terminated by fixing cells 21 hours after irradiation (pulsed conditions, t_1) or 12 hours after irradiation (sustained conditions, t_2) and probing for expression of *CDKN1A* or *PML* by means of FISH. (**E**) *CDKN1A* and (**F**) *PML* expression versus cumulative p53 in individual cells. a.u., arbitrary units; r.f.u., relative fluorescence units (supplementary materials). (**G**) Model for p53 dynamics controlling cell fate. Transient damage encountered under low-radiation dose or physiological conditions is repaired quickly and generates a small number of p53 pulses, allowing the cell to continue dividing. Persistent damage—whether from a large number of initial DNA lesions or a small number of irreparable breaks—generates repeated p53 pulses that ultimately trigger cellular senescence. t_1 and t_2 represent time points in which the cumulative level of p53 is equal between pulsed and sustained conditions. However, the probability of entering senescence differs between these two types of dynamics. Pulsed p53 allows more time for recovery from DNA damage, whereas sustained p53 accelerates this process.

References and Notes

1. L. Cai, C. K. Dalal, M. B. Elowitz, *Nature* **455**, 485 (2008).
2. N. Hao *et al.*, *Mol. Cell* **30**, 649 (2008).
3. A. Hoffmann, A. Levchenko, M. L. Scott, D. Baltimore, *Science* **298**, 1241 (2002).
4. G. Lahav *et al.*, *Nat. Genet.* **36**, 147 (2004).
5. J. T. Mettetal, D. Muzzey, C. Gómez-Uribe, A. van Oudenaarden, *Science* **319**, 482 (2008).
6. D. E. Nelson *et al.*, *Science* **306**, 704 (2004).
7. G. M. Süel, J. Garcia-Ojalvo, L. M. Liberman, M. B. Elowitz, *Nature* **440**, 545 (2006).
8. S. Tay *et al.*, *Nature* **466**, 267 (2010).
9. J. J. Ventura *et al.*, *Mol. Cell* **21**, 701 (2006).
10. T. K. Lee *et al.*, *Sci. Signal.* **2**, ra65 (2009).
11. S. L. Werner, D. Barken, A. Hoffmann, *Science* **309**, 1857 (2005).
12. S. D. Santos, P. J. Verveer, P. I. Bastiaens, *Nat. Cell Biol.* **9**, 324 (2007).
13. L. Ashall *et al.*, *Science* **324**, 242 (2009).
14. R. E. Dolmetsch, K. Xu, R. S. Lewis, *Nature* **392**, 933 (1998).
15. M. H. Sung *et al.*, *PLoS ONE* **4**, e7163 (2009).
16. N. Hao, E. K. O'Shea, *Nat. Struct. Mol. Biol.* **19**, 31 (2012).
17. L. O. Murphy, S. Smith, R. H. Chen, D. C. Fingar, J. Blenis, *Nat. Cell Biol.* **4**, 556 (2002).
18. H. F. Horn, K. H. Vousden, *Oncogene* **26**, 1306 (2007).
19. B. Vogelstein, D. Lane, A. J. Levine, *Nature* **408**, 307 (2000).
20. E. Batchelor, A. Loewer, C. Mock, G. Lahav, *Mol. Syst. Biol.* **7**, 488 (2011).
21. N. Geva-Zatorsky *et al.*, *Mol. Syst. Biol.* **2**, 2006, 0033 (2006).
22. D. A. Hamstra *et al.*, *Cancer Res.* **66**, 7482 (2006).
23. W. Hu *et al.*, *Cancer Res.* **67**, 2757 (2007).
24. R. Lev Bar-Or *et al.*, *Proc. Natl. Acad. Sci. U.S.A.* **97**, 11250 (2000).
25. A. Loewer, E. Batchelor, G. Gaglia, G. Lahav, *Cell* **142**, 89 (2010).
26. E. Batchelor, C. S. Mock, I. Bhan, A. Loewer, G. Lahav, *Mol. Cell* **30**, 277 (2008).
27. R. Zhao *et al.*, *Genes Dev.* **14**, 981 (2000).
28. L. T. Vassilev *et al.*, *Science* **303**, 844 (2004).
29. C. Tovar *et al.*, *Proc. Natl. Acad. Sci. U.S.A.* **103**, 1888 (2006).
30. T. Riley, E. Sontag, P. Chen, A. Levine, *Nat. Rev. Mol. Cell Biol.* **9**, 402 (2008).
31. E. de Stanchina *et al.*, *Mol. Cell* **13**, 523 (2004).
32. K. D. Kelley *et al.*, *Cancer Res.* **70**, 3566 (2010).
33. J. Campisi, F. d'Adda di Fagagna, *Nat. Rev. Mol. Cell Biol.* **8**, 729 (2007).
34. F. d'Adda di Fagagna, *Nat. Rev. Cancer* **8**, 512 (2008).
35. A. M. Bode, Z. Dong, *Nat. Rev. Cancer* **4**, 793 (2004).

Acknowledgments: We thank R. Agami for the MCF7/p53shRNA cell line; B. Fang for the MCF7/Casp3 cell line; A. Raj and Z. Waks for help with mRNA FISH; R. Kishony, R. Ward, W. Forrester, E. O'Shea, T. Mitchison, A. Klein, J. Orth, and U. Alon for comments and discussions; and the Nikon Imaging Center at Harvard Medical School for help with light microscopy. This research was supported by the Novartis Institutes for Biomedical Research, the National Institutes of Health grant GM083303 and fellowship F32GM095168 (J.E.P), a National Science Foundation graduate fellowship (K.W.K), the American Cancer Society, California Division, Pamela and Edward Taft Postdoctoral Fellowship (E.B.), and fellowships from the German Research Foundation and the Charles A. King Trust (A.L.). J.E.P and G.L. conceived the study, designed the experiments, and wrote the paper. J.E.P modeled and designed perturbation experiments and performed gene expression and cell fate assays, live-cell microscopy, single-cell mRNA detection, and image analysis. K.W.K. performed live-cell microscopy, single-cell mRNA detection, and image analysis. C.M. characterized p53 and p53-Venus dynamics under radiation and various drug treatments. E.B. and A.L. performed UV treatment experiments and provided preliminary results and foundational concepts.

Supplementary Materials

www.sciencemag.org/cgi/content/full/336/6087/1440/DC1
Materials and Methods
Figs. S1 to S8
Tables S1 to S5
References (*36*, *37*)

22 December 2011; accepted 1 May 2012
10.1126/science.1218351

p53 Dynamics Control Cell Fate

Jeremy E. Purvis *et al.*

Science **336**, 1440 (2012);
DOI: 10.1126/science.1218351